Max-Planck-Institut
für Mathematik
in den Naturwissenschaften
Leipzig

Surface structure of ferroelastic domain walls: a continuum elasticity approach

by

Sergio Conti and Ekhard K. H. Salje

Preprint no.: 27 2001

Surface structure of ferroelastic domain walls: a continuum elasticity approach

Sergio Conti† and Ekhard K H Salje‡

† Max-Planck-Institute for Mathematics in the Sciences,
Inselstr. 22-26, D 04103 Leipzig, Germany
‡ Dept. of Earth Sciences, University of Cambridge
Downing Street, Cambridge CB2 3EQ, UK

15.5.2001

Abstract. We present a model based on continuum elasticity and energy minimization for the study of ferroelastic domain walls close to a surface. We focus on walls orthogonal to the surface, and predict a double-peak structure in the surface values of the squared elastic strain, which is directly related to the chemical reactivity. We also compute the height profile, which can be measured, in principle, e.g. with AFM, and the strain distribution in the bulk. Our results are in good agreement with previous atomistic simulations, which had required much bigger computational effort. Our approach is also used to explore the effect of the cubic anisotropy (C_{12}/C_{11}) on the surface structure of the intersection between the twin wall and the crystal surface.

1. Introduction

Domain walls offer a rare opportunity to selectively dope two-dimensional sections in the bulk of crystalline materials. The enhanced chemical reactivity of the elastically strained region around the domain wall has been demonstrated experimentally, and has been used to form two-dimensional superconducting regions in an insulating matrix [1, 2]. The process of selective doping is in large part controlled by the elastic strains present in the material, and by their interaction with surface relaxation, which is still poorly understood.

Spontaneous formation of microstructure in bulk ferroelastic materials under cooling below the transition temperature is well understood from a thermodynamic point of view [3]. Existing theories focus on average properties and do not provide a precise local description of the microstructure, except for few characteristics, such as the one-dimensional profile of flat domain walls in the bulk, for which the long-standing theoretical predictions have recently been confirmed experimentally by X-ray scattering [4, 5]. The resulting picture, at least in oxide ferroelastics, is that of a smooth change of the order parameter from one value to the other, over a distance of many unit cells, which is well described by continuum theories.

Much less attention has been devoted to surface relaxation effects. It may be expected that the ferroelastic order parameter is reduced close to a surface, suggesting local deformations in the surface layer comparable to those found in the interior of the domain wall. Theoretical models for the surface relaxation indicate the possibility of oscillations on the unit-cell scale close to the surface [6, 7] in some parameter ranges.

The interaction of the wall structure with surface relaxation necessarily generates two-dimensional patterns, which are relevant both for real-space probing of the material properties, e.g. via atomic force microscopy [8], and for interacting with the material, e.g. via doping [1, 2, 9]. Domain walls constitute a region of higher chemical reactivity inside the material, and are a natural candidate for selective doping.

The surface structure of domain walls has been first studied theoretically by Novak and Salje [10, 11] who performed extensive numerical simulations of a two-dimensional atomistic model, chosen to represent typical perovskite elastic properties. They predicted that the resulting elastic strains generate a complex pattern, which includes a thinning of both the domain wall and the surface relaxation around their intersection, and a double-peak structure in the surface values of the square of the order parameter. However, the large computational effort required by their atomistic computations prevented an analysis of the dependence of the results on the material parameters, including the assessment of the robustness of such features with respect to parameter changes. Further, their method is unpractical for application to specific materials, due to the extremely high number of atoms which are present in such two-dimensional structures. In this paper we present a continuum, linearly elastic model which captures the essential features of their results without requiring large numerical effort for the solution. We are thus able to study the material behaviour in function of material parameters, and observe that the double-peak structure observed by Novak and Salje is a signature of cubic anisotropy, which was very strong in their model. In approximately isotropic materials instead we predict a different pattern, with much stronger effects on the surface height profiles, but smoother order-parameter distributions. Except for the bulk elastic constants, which are at least approximately known for most materials, our model has only two parameters, the wall width and the strength of surface relaxation. We expect this model to be applicable to real-world problems, with experimentally determined material parameters.

2. Model

We consider a cubic material which undergoes a C_{44} shear instability. We restrict to two variants separated by a single domain wall, and reduce to two spatial dimensions assuming that the geometry is invariant under translations in the third one. Let the material occupy the $y \geq 0$ half-plane, and the domain wall be located on $x = 0$. This fixes the phase distribution, and allows us to replace the nonconvex elastic potential with a (phase-dependent) convex one, which for simplicity we take to be quadratic. Since the ferroelastic transition corresponds to a small shear deformation, we take all

elastic constants to be those of the parent cubic phase, except of course the unstable one, C_{44}. This amounts to reducing the number of independent constants to those of a cubic crystal, and leads to

$$W_b(\nabla u, x) = \frac{1}{2}C_{11}(u_{x,x}^2 + u_{y,y}^2) + C_{12}u_{x,x}u_{y,y} + \frac{1}{2}C_{44}(u_{x,y} + u_{y,x} - 2\alpha)^2 \tag{1}$$

where $\alpha(x) = |\alpha|\mathrm{sgn}(x)$ is the spontaneous shear. The C_{44} constant is very small around the transition, and indeed it vanishes at second-order transition points [12]. Whereas in isotropic materials $C_{11} = C_{12}$, the perovskites in which we are interested have a significant cubic anisotropy, due to the strong metal-oxygen bonds. We shall consider the range $0 \leq C_{12} \leq C_{11}$, $C_{44} \ll C_{11}$. For comparison, the linearization of the discrete Novak-Salje model [10, 11] delivers $C_{11} \simeq 2800$, $C_{12} \simeq C_{44} \simeq 1$.

The spontaneous strain is reduced at the surface. To model this effect, we use a different elastic energy in the surface region with respect to the bulk. Whereas the reduced symmetry along the surface would in principle allow for a variety of different terms, in practice, only C_{44} is relevant for the present purposes. We choose

$$W_s(\nabla u) = \frac{1}{2}\gamma C_{44}(u_{x,y} + u_{y,x})^2 \,. \tag{2}$$

Here, γ represents the relative strength of the surface relaxation, and the minimum of W_s has been set at zero shear for simplicity. More general (but still quadratic) expressions for W_s can be included in the present formalism without any change, however the little available knowledge of the material parameters entering such energies limits the usefullness of more complex expressions.

Finally, the microscopic length scale ϵ, which represents the wall thickness (and, as we shall see, the surface relaxation length as well), enters the energy though the simplest second-order singular perturbation, the squared norm of the second gradient $\epsilon^2|\nabla^2 u|^2$. The full energy is then

$$E[u] = \int_{\{y>0\}} W_b(\nabla u) + \frac{1}{2}C_{44}\epsilon^2|\nabla^2 u|^2 \, dxdy + \int_{\{y=0\}} \epsilon W_s(\nabla u)\, dx \,, \tag{3}$$

where the coefficient ϵ in front of the surface term arises because W_s is active only in a small strip around the surface, whose width is of the order of the microscopic length scale ϵ (this makes γ an adimensional parameter). The coefficient $C_{44}/2$ in front of the ϵ^2 term has been chosen for convenience, so that ϵ has the dimensions of length and coincides with the decay length of domain walls (see below).

The symmetry of the problem under reflections with respect to the domain wall $\{x = 0\}$ allows us to restrict attention to the first quadrant. Continuity of ∇u and simmetry give then the boundary conditions

$$u_x = u_{y,x} = 0 \qquad\qquad \text{for } x = 0 \,. \tag{4}$$

From now on, equations shall be specialized to the first quadrant, and $\alpha = |\alpha|$ will always take the positive value (results for the second quadrant are obtained by changing a few signs). In the numerical results we shall use ϵ as unit of length, α as unit of deformation,

and C_{44} as unit of energy (in the present linear approach deformations can be scaled independently of lengths).

In the rest of this paper we analyze the shape of the minimizers of (3) for various values of the parameters, in the given geometry. We start with the surface relaxation. In the bulk of the system the minimizer is $u^b(x,y) = (0, 2\alpha x)$. Approaching the surface $\{y = 0\}$, we seek a solution such that the perturbation is invariant under translations in x, i.e. of the form $u^s(x,y) = u^b(x) + w(y)$. Explicit minimization gives

$$u^s(x,y) = 2\alpha \begin{pmatrix} \epsilon \frac{\gamma}{\gamma+1} \mathrm{e}^{-y/\epsilon} \\ x \end{pmatrix} . \tag{5}$$

which does not depend on the elastic constants C_{11} and C_{12}. The value of the order parameter on the surface

$$\left. \frac{u^s_{x,y} + u^s_{y,x}}{2} \right|_{y=0} = \frac{\alpha}{\gamma+1} \tag{6}$$

turns out to be reduced by a factor $\gamma + 1$ with respect to the bulk value, providing a physical interpretation for the parameter γ.

We now turn to the domain wall. Away from the surface, its structure is invariant under translations in y, hence we seek $u^w(x,y) = u^w(x)$ which obeys (4) at $x = 0$ and approaches u^b at large x. We obtain

$$u^w(x) = \begin{pmatrix} 0 \\ 2\alpha(x + \epsilon \mathrm{e}^{-x/\epsilon}) \end{pmatrix} \tag{7}$$

(the parameter ϵ is, hence, physically equivalent to the 'wall thickness' parameter w in Landau-Ginzburg theory [3]). For $x = 0$ the order parameter is obviously 0. The second derivative $u_{y,xx}$ is discontinuous at $x = 0$. This is due to the linearization of W_b around the two minima, and would be absent for a smooth, nonconvex W_b.

From a qualitative point of view, the strain field at the intersection of surface and interface is generated because the boundary condition given in Equation (4), $u_x(0,y) = 0$, is incompatible with the surface relaxation u^s computed in Equation (5). This incompatibility has to be accomodated by elastic deformation. We can get a rough idea of the resulting strain patterns, in the relevant $C_{11} \gg C_{44}$ case, by assuming uniform relaxation of the strain in a region of size $(0,\xi) \times (0,\epsilon)$. From Equation (5), the mismatch $u_x(0,y)$ is of order $g = \alpha\epsilon\gamma/(\gamma+1)$. Hence, $u_{x,x} \simeq g/\xi$ and $\delta u_{x,y} \simeq g$. The strain enerty is then $C_{11}\delta u^2_{x,x}\xi + C_{44}\alpha^2\xi\epsilon \simeq \epsilon^2\alpha^2(C_{11}/\xi + C_{44}\xi)$, giving $\xi \sim (C_{11}/C_{44})^{1/2}$ (the second-gradient bending term is of lower order, since $\xi \gg \epsilon$). This computation assumes that no additional strains are developed in the y direction, which is correct if $C_{12} \ll C_{11}$. If $C_{12} \simeq C_{11}$ instead, it is convenient to rewrite W_b as

$$W_b(\nabla u, x) = \frac{1}{2}C_{11}(u_{x,x} + u_{y,y})^2 - (C_{11} - C_{12})u_{x,x}u_{y,y} + \frac{1}{2}C_{44}(u_{x,y} + u_{y,x} - 2\alpha)^2 \tag{8}$$

which emphasizes the softening of the $u_{y,y} = -u_{x,x}$ mode. In this case the deformation can be accomodated by volume-preserving transformations which couple only to the small energy coefficients C_{44} and $C_{11} - C_{12}$. The length scale is then $\xi \simeq \epsilon$.

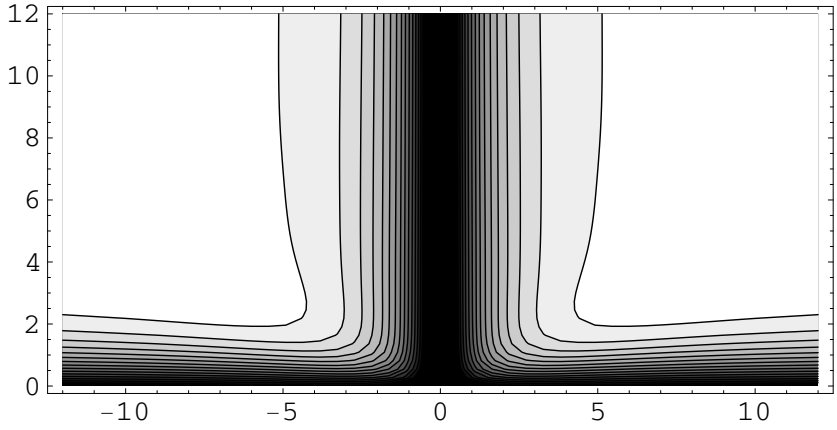

Figure 1. Contour plot of the absolute value of the order parameter $|e_{xy}|$ for $C_{11} = 100C_{44}$, $C_{12} = 0$ and $\gamma = 2$. All curves come closer to the x-axis around $x \sim 3$, the two higher ones (the most internal ones) also approach the y-axis.

3. Numerical solution

In order to solve numerically our model, we first obtain an analytic approximate solution u^0 which satisfies the boundary conditions [Equation (4)], the asymptotic behaviours at large x [Equation 5)] and at large y [Equation (7)], then expand the difference in a set of localized basis functions,

$$u(x,y) = u^0(x,y) + \sum_n c_n u^{(n)}(x,y)\,. \tag{9}$$

The approximate solution we chose, which is obtained combining (5) and (7), is

$$u^0(x,y) = 2\alpha \begin{pmatrix} \epsilon\frac{\gamma}{\gamma+1}\mathrm{e}^{-y/\epsilon}(1-\mathrm{e}^{-x/\epsilon}) \\ x + \epsilon\mathrm{e}^{-x/\epsilon} \end{pmatrix}\,. \tag{10}$$

The localized basis is composed by polynomials and exponentials,

$$u^{(n)}(x,y) = e^{(n)} x^{a_n} y^{b_n} \exp\left\{-\frac{x}{\lambda_n} - \frac{y}{\mu_n}\right\}\,. \tag{11}$$

Here, $e^{(n)}$ is the polarization vector, i.e. a unit vector in the $\hat{x}$ or $\hat{y}$ direction, a_n and b_n are nonnegative integers, λ_n and μ_n positive constants. The values of $e^{(n)}$, a_n, b_n, λ_n and μ_n are fixed a priori, with λ_n and μ_n chosen to reproduce the length scales which we expect to be present in the solution. The qualitative analysis above suggests that it is useful to include some λ_n of order $\epsilon\sqrt{C_{44}/C_{11}}$, some of order ϵ and some of order $\epsilon\sqrt{C_{44}/C_{11}}$. The boundary condition (4) is implemented avoiding all functions with $a_n = 0$, and replacing x with $(x + \lambda_n)$ in those with $a_n = 1$, $\mathbf{e}^{(n)} = \hat{y}$. All integrals appearing in the energy (3) can be reduced to sums of monomials times decaying exponentials, hence can be done analytically. The resulting quadratic problem in the coefficients c_n can be then solved numerically using standard linear-algebra packages. We used both LU Decomposition and Singular Value Decomposition from [13], with no appreciable difference. Increasing

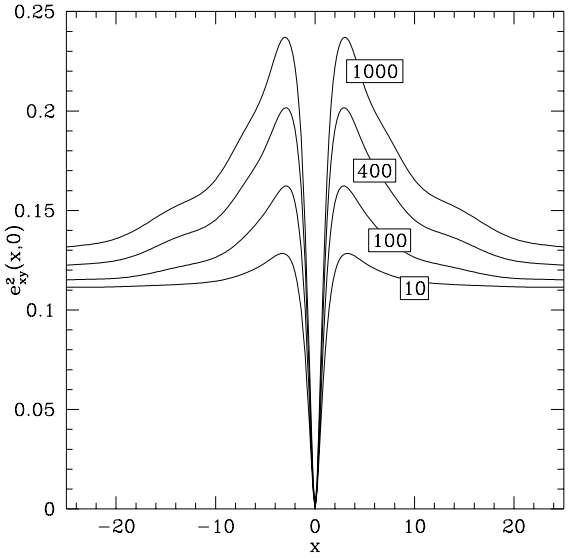

Figure 2. Squared order parameter e^2_{xy} as a function of x at $y = 0$ for $C_{12} = 0$, $\gamma = 2$ and $C_{11}/C_{44} = 1000$, 400, 100 and 10 (from upper to lower curve).

the number of basis functions gives a systematic way to improve the results and to control convergence. In practice, we used a basis of around 300 vectors.

Figure 1 displays a contour plot of the absolute value of the order parameter $e_{xy} = (u_{x,y} + u_{y,x})/2$ for $C_{11} = 100C_{44}$, $C_{12} = 0$ and $\gamma = 2$. This choice of γ corresponds to a reduction by a factor of 3 of the order parameter on the surface, which is the same used in the atomistic simulations by Novak and Salje. The choice $C_{12} = 0$ corresponds to a very strong cubic anisotropy, this however does not strongly influence the results, see below. Finally, the large value of C_{11}/C_{44} corresponds to the softness of the active mode close to the transition temperature, and is the main large parameter that determines the aspect of the solution.

Figure 1 shows that both the wall width and the surface relaxation depth are reduced near their intersection. The same fact can be seen by plotting the squared order parameter on the surface, which is directly related to the chemical reactivity of the material. Figure 2 shows $e^2_{xy}(x, 0)$ for various values of C_{11}. It is evident that the double-peak structure, corresponding to the reduction of the surface relaxation displayed in Figure 1, is more prominent for large C_{11}/C_{44}. The role of C_{12} is analyzed in Figure 3, for fixed C_{11}/C_{44}. Whereas the double-peak is almost absent in the isotropic case $C_{11} = C_{12}$, it is clearly present already with a 20% reduction in C_{12} with respect to C_{11}, which corresponds to a moderate cubic anisotropy, and its height does not sensibly depend on C_{12} in the regime $0 \leq C_{12}/C_{11} \leq 1/2$. The disappearence of the peak for $C_{12} \simeq C_{11}$ corresponds to the softening of the shear mode $u_{x,x} - u_{y,y}$ [see Equation (8)].

The role of γ is investigated in Figure 4. Since the order parameter on the surface scales as $(\gamma + 1)^{-1}$, we plot the normalized values $e^2_{xy}(\gamma + 1)^2$. The relative importance

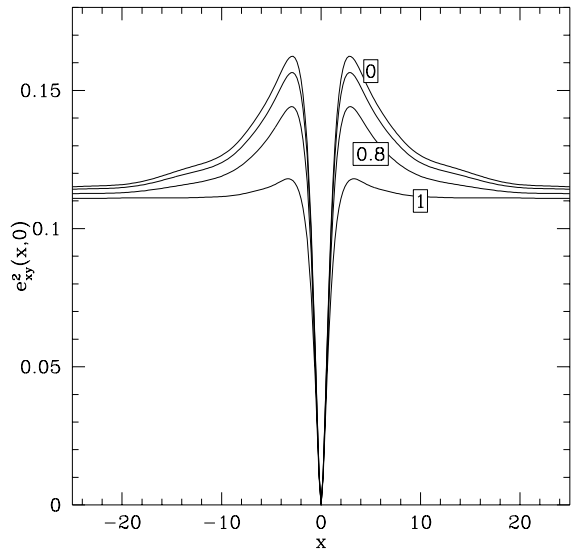

Figure 3. Squared order parameter e^2_{xy} as a function of x at $y = 0$ for $C_{11}/C_{44} = 100$ and $C_{12}/C_{11} = 0$, 0.5, 0.8 and 1 (from upper to lower curve).

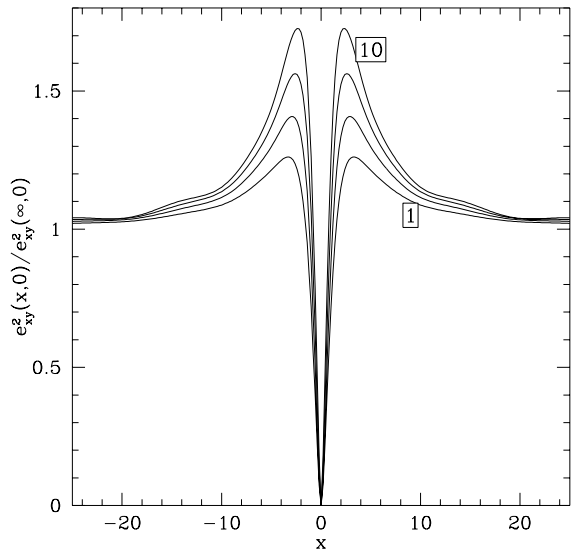

Figure 4. Squared rescaled order parameter $e^2_{xy}(x,0)/e^2_{xy}(\infty,0)$ as a function of x for $C_{11}/C_{44} = 100$ and $C_{12}/C_{11} = 0.5$, for $\gamma = 10$, 4, 2 and 1 (from upper to lower curve).

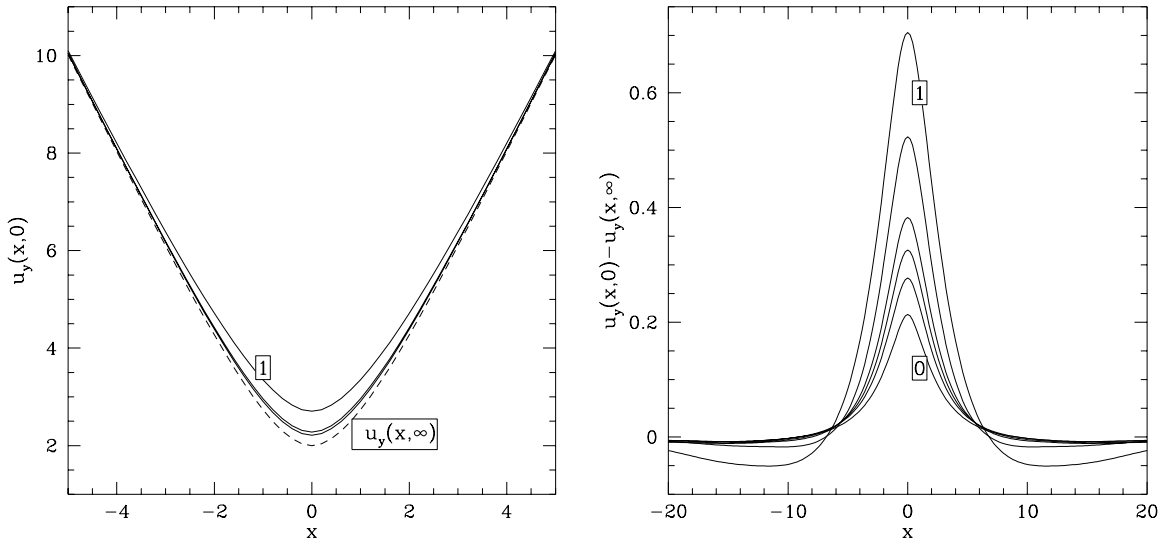

Figure 5. Left panel: Surface topography $u_y(x,0)$ for $C_{11} = 100C_{44}$, $\gamma = 2$, and $C_{12}/C_{11} = 1,\ 0.8,\ 0$ (from top to bottom, the two lower curves are barely distinguishable), compared with the unrelaxed wall profile $u_y(x,\infty)$ (dashed curve). Right panel: surface topography referred to the bulk wall profiles, $u_y(x,0) - u_y(x,\infty)$, for $C_{12}/C_{11} = 1,\ 0.99,\ 0.95,\ 0.9,\ 0.8$, and 0 (from higher to lower curve at $x = 0$) .

of the peak increases with increasing γ. This effect is however rather small in absolute values, since for example at $\gamma = 10$ even at the peak $e_{xy}(x,0)$ reaches only about 10% of its bulk value.

Figure 5 displays the resulting surface topography, as an absolute value and as difference with the bulk value $u(x,\infty)$ (which corresponds to the result without surface relaxation, i.e. with $\gamma = 0$). In all the considered cases the part of the domain wall close to the surface is contracted in the y-direction, leading to an additional smoothing of the corner. Qualitatively, this can be attributed to the tensile stresses present on the surface, as discussed at the end of Section 2. As a consequence, we see that measuring the height of the surface as an estimate of the wall profile will underestimate the curvature in the central region. This effect is particularly pronounced in the case $C_{11} = C_{12}$, where the presence of an additional soft mode leads to a much larger relaxation. Indeed, in the latter case the dilative $u_{x,x}$ strain due to the surface relaxation is relaxed via the shear $u_{x,x} - u_{y,y}$ channel, resulting in stronger compression along $u_{y,y}$.

Acknowledgements

Interesting discussions with Gero Friesecke, Stefan Müller, Jurica Novak, and Florian Theil are gratefully acknowledged. This work was partially supported by the EU TMR network *"Phase Transitions in Crystalline Solids"*, contract. no. FMRX-CT98-0229.

References

[1] Aird A and Salje E K H 1998 *J. Phys.: Condens. Matter* **10** L377
[2] Reich S and Tsabba Y 1999 *Eur. Phys. J. B* **9** 1
[3] Salje E K H 1990 *Phase transitions in ferroelastic and co-elastic crystals* (Cambridge: Cambridge University Press)
[4] Locherer K R, Hayward S A, Hirst P J, Chrosch J, Yeadon M, Abell J S and Salje E K E 1996 *Phil. Trans. R. Soc. Lond. A* **354** 2815
[5] Locherer K R, Chrosch J and Salje E K E 1998 *Phase Transitions* **67** 51
[6] Houchmandzadeh B, Lajzerowicz J and Salje E K H 1992 *Phase Transitions* **38** 77
[7] Houchmandzadeh B, Lajzerowicz J and Salje E K H 1992 *J. Phys.: Condens. Matter* **4** 9779
[8] Bosbach D, Putnis A, Bismayer U and Güttler B 1997 *J. Phys.: Condens. Matter* **9** 8397
[9] Aird A and Salje E K H 2000 *Eur. Phys. J. B* **15** 205
[10] Novak J and Salje E K H 1998 *Eur. Phys. J. B* **4** 279
[11] Novak J and Salje E K H 1998 *J. Phys.: Condens. Matter* **10** L359
[12] Carpenter M A and Salje E K H 1998 *Eur. J. Mineral.* **10** 693
[13] Press W H, Teukolsky S A, Vetterling W T and Flannery B P 1992 *Numerical Recipes in C: the art of scientific computing* 2nd ed. (Cambridge: Cambridge University Press)